



## Benzamide derivatives as dual-action hypoglycemic agents that inhibit glycogen phosphorylase and activate glucokinase

Lei Zhang<sup>a,†</sup>, Honglin Li<sup>b,†</sup>, Qingzhang Zhu<sup>a,†</sup>, Jun Liu<sup>c</sup>, Ling Chen<sup>a</sup>, Ying Leng<sup>a,\*</sup>, Hualiang Jiang<sup>a,b</sup>, Hong Liu<sup>a,\*</sup>

<sup>a</sup>State Key Laboratory of Drug Research, Shanghai Institute of Materia Medica, Shanghai Institutes for Biological Sciences, Chinese Academy of Sciences, 555 Zu Chong Zhi Road, Shanghai 201203, PR China

<sup>b</sup>School of Pharmacy, East China University of Science and Technology, Shanghai 200237, PR China

<sup>c</sup>Jiangsu Center for Drug Screening, China Pharmaceutical University, Nanjing 210038, PR China

### ARTICLE INFO

#### Article history:

Received 17 July 2009

Revised 19 August 2009

Accepted 20 August 2009

Available online 24 August 2009

#### Keywords:

Glucokinase (GK) activators

Glycogen phosphorylase (GP) inhibitors

Type 2 diabetes

Dual action

### ABSTRACT

A series of benzamide derivatives which can simultaneously inhibit glycogen phosphorylase (GP) and activate glucokinase (GK) were prepared and evaluated. The structure–activity relationships (SAR) of these compounds were also presented. Among these, compounds **12**, **13l**, **13q**, and **13v** showed moderate activities towards both GK and GP. Compound **13h** inhibited hLGP with an IC<sub>50</sub> of 8.95 μM and activated GK with an EC<sub>50</sub> of 1.87 μM. The possible binding modes of compounds **12**, **13l**, **13h**, and **13q** with GP and GK were also explored by molecular docking simulation.

© 2009 Elsevier Ltd. All rights reserved.

### 1. Introduction

Abnormal glucose metabolism is the major pathologic factor of Type 2 diabetes mellitus. Elevated hepatic glucose production (HGP) by glycogenolysis and gluconeogenesis is a contributing factor to hyperglycemia.<sup>1</sup> Therefore enzymes that have high control strength on hepatic glucose metabolism are potential targets for controlling hepatic glucose balance and thereby modulating blood glucose levels in Type 2 diabetes. Glucokinase (GK) and glycogen phosphorylase (GP), two critical enzymes involved in the process of glucose metabolism, have high control strength over glucose metabolism (Fig. 1). And both of them are potential therapeutic targets for Type 2 diabetes.

Glucokinase (hexokinase IV or D) is a cytoplasmic enzyme that phosphorylates glucose and triggers glucose utilization and metabolism. It is predominantly expressed in liver and pancreas, where it removes glucose from the blood and reacts with adenosine triphosphate (ATP) to form glucose-6-phosphate (Glu-6-P), the first and rate-limiting biosynthetic step in the conversion of glucose to its storage form, glycogen.<sup>2</sup> Phosphorylation of glucose by GK in the liver promotes glycogen synthesis, while in the pancreatic β-cell this results in glucose-sensitive insulin release.<sup>3</sup> Both of these effects in turn reduce plasma glucose levels. Therefore, acti-

vation of GK is expected to improve glycemic control by modulating hepatic glucose balance and decreasing the threshold for insulin secretion. Several groups have described various synthetic small molecules that act as GK activators, which function through binding to an allosteric site (Fig. 2).<sup>4</sup> Among these, Banyu company has identified a small synthetic compound **6** as GK activator and published its crystal structure bound to GK.<sup>5</sup>

Glycogen phosphorylase, the rate determining enzyme of glycogen degradation, catalyzes the breakdown of glycogen to glucose-1-phosphate.<sup>6</sup> In the liver glucose-1-phosphate is metabolised further to glucose, which is then secreted into the bloodstream. GP exists in two interconvertible forms, GP<sub>a</sub> (the phosphorylated form, high activity, high substrate affinity, predominantly R state) and GP<sub>b</sub> (the nonphosphorylated form, low activity, low substrate affinity, predominantly T state).<sup>7</sup> So inhibition of GP<sub>a</sub> may represent another useful therapy for the treatment of Type 2 diabetes. Several structurally different classes of small molecule inhibitors have been reported (Fig. 3).<sup>8–10</sup> Based on screening of specs library and structural modification, we have recently described a series of benzamide derivatives as GP inhibitors, among which compound **12** showed a moderate rabbit muscle GP<sub>a</sub> inhibitory activity with an IC<sub>50</sub> of 2.68 μM.<sup>11</sup>

Obviously, GP<sub>a</sub> inhibitor **12** bears a similar structure with GK activator **6** because both of them share a tetra-substituted benzamide scaffold with a heteroaryl thiol moiety. Thus we speculate that this kind of compounds can play a dual-action role as hypoglycemic agents that not only inhibit glycogen phosphorylase

\* Corresponding authors. Tel.: +86 21 50807042; fax: +86 21 50807088 (H.L.).

E-mail address: [hliu@mail.shcnc.ac.cn](mailto:hliu@mail.shcnc.ac.cn) (H. Liu).

† Authors equally contributed to this work.

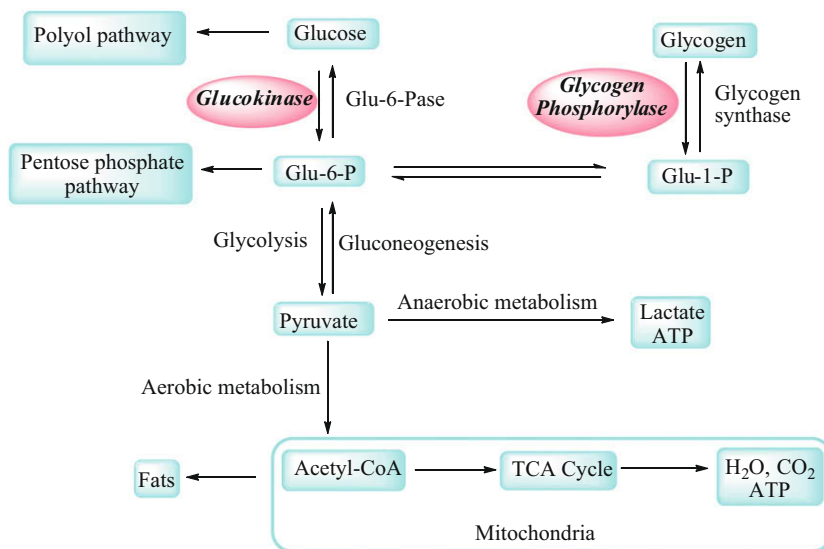


Figure 1. Simplified glucose metabolism pathway.

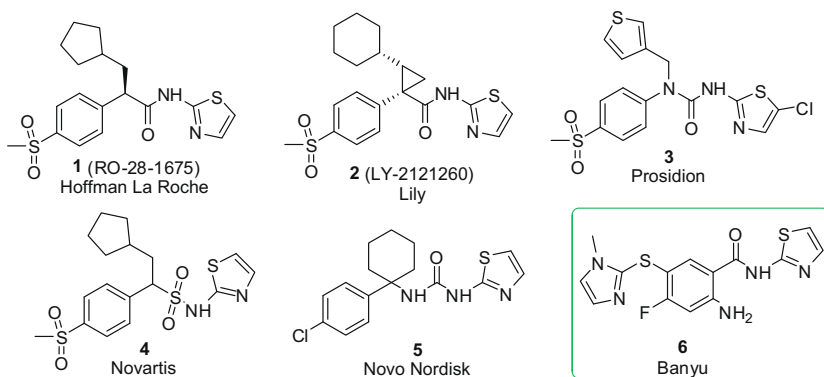


Figure 2. Structures of representative GK activators.

but also activate glucokinase. It has been reported that CP-320626 developed by Pfizer was a dual-action hypoglycemic and hypocholesterolemic agents that inhibited glycogen phosphorylase and lanosterol demethylase, which had the potential to favorably affect both hyperglycemia and hypercholesterolemia in patients with Type 2 diabetes.<sup>12</sup> To verify our hypothesis, we firstly carried out biological evaluation of compound **6** towards both GK and GP. As expected, compound **6** showed moderate GP<sub>a</sub> inhibitory efficacy (GP<sub>a</sub> IC<sub>50</sub> = 43.9 μM) as well as good GK activating efficacy (GK EC<sub>50</sub> = 0.06711 μM).

Then we continued our structure–activity relationship (SAR) efforts around compound **12**. A series of benzamide compounds as well as piperazine-containing amides and symmetrical benzamide analogues were designed and synthesized, and their biological activities towards both GK and GP were evaluated. Among these, compounds **12**, **13i**, and **13q** showed moderate activity towards both GK and GP. Compound **13h** inhibited GP<sub>a</sub> with an IC<sub>50</sub> of 8.95 μM and activated glucokinase with an EC<sub>50</sub> of 1.87 μM. The possible binding modes of compounds **12**, **13i**, **13h**, and **13q** with glycogen phosphorylase a and glucokinase were also explored by molecular docking simulation.

## 2. Chemistry

As part of our SAR studies around compound **12**, compounds **13a–x** were designed and synthesized. In general, treatment of 4,

5-difluoro-2-nitrobenzoic acid with oxalyl dichloride and DMF afforded 4, 5-difluoro-2-nitrobenzoyl chloride **16**. Then **16** reacted with appropriate commercially available aniline to give benzamides **17a–x**. Reaction of **17a–x** with corresponding thiols and triethylamine provided **18a–x**. And compounds **13a–x** were obtained by hydrogenising **18a–x** catalyzed by iron powder and saturated aqueous NH<sub>4</sub>Cl (Scheme 1).

The series of piperazine-containing amide analogues **14a–e** were prepared from 1-(2-*R*<sub>2</sub>-phenyl) piperazine and **19a–e** which were produced by the reaction of 2-chloroacetyl chloride with amino compounds as shown in Scheme 2.

The series of symmetrical benzamide analogues **15a–c** were synthesized by isophthaloyl dichloride reacting with aniline in the presence of pyridine or triethylamine as shown in Scheme 3.

## 3. Biology

### 3.1. Glucokinase enzyme assays

cDNA of human glucokinase (MGC: 1742, purchased from OriGene Technologies, USA) was subcloned into the pET28a(+) expression vector, and expressed in *Escherichia coli* strain BL21(DE3).<sup>13–15</sup> The NH<sub>2</sub> terminal end of (His)<sub>6</sub>-tag glucokinase fusion protein was purified by Ni-NTA metal chelate affinity chromatography and stored at –80 °C in 50 mM Tris–HCl pH7.4, 1 mM DTT, 50 mM NaCl and 10% glycerol.<sup>16</sup>

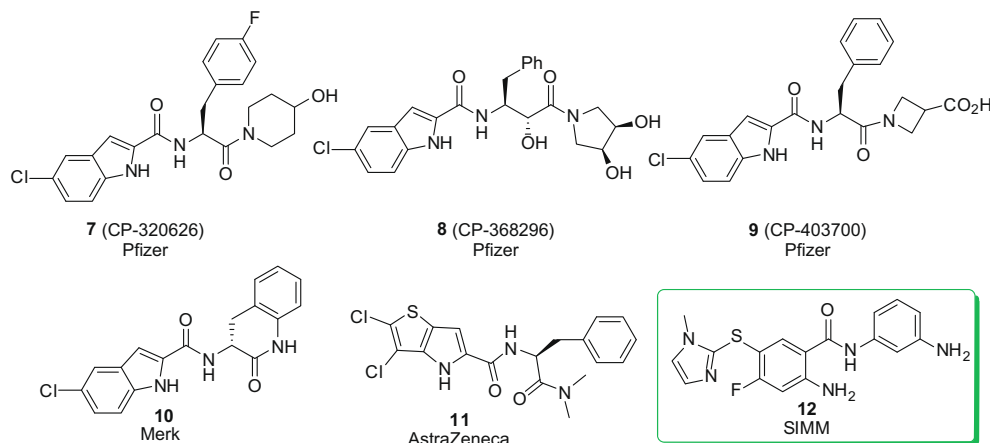
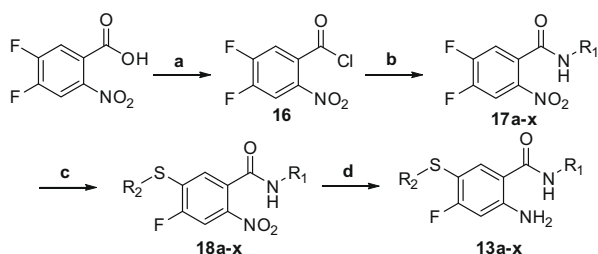
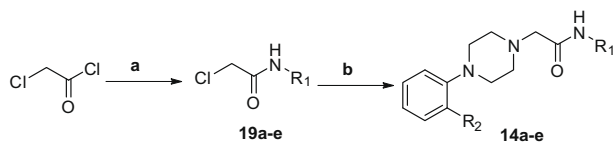


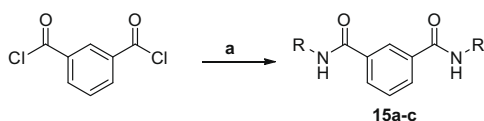
**Figure 3.** Selected inhibitors binding at the interface of the GP homodimer.



**Scheme 1.** Reagents and conditions: (a) oxalyl chloride (1.2 equiv), DMF (two drops),  $\text{CH}_2\text{Cl}_2$ , rt, 2 h; (b)  $\text{R-NH}_2$  (1 equiv), pyridine (2 equiv),  $\text{CH}_2\text{Cl}_2$ , rt; (c) thiol (1 equiv),  $\text{Et}_3\text{N}$  (3 equiv),  $\text{CH}_3\text{CN}$ , mw,  $80^\circ\text{C}$ , 40 min; (d) iron powder (10 equiv), isopropanol, reflux, 0.5 h.



**Scheme 2.** Reagents and conditions: (a)  $\text{R}_1\text{-NH}_2$  (1 equiv),  $\text{K}_2\text{CO}_3$  (2 equiv), THF,  $45^\circ\text{C}$ , 2 h; (b) 1-(2- $\text{R}_2$ -phenyl)piperazine (1 equiv), KI (catalyzer),  $\text{K}_2\text{CO}_3$  (2 equiv), THF,  $50^\circ\text{C}$ , 4 h.



**Scheme 3.** Reagents and conditions: (a)  $\text{NH}_2\text{-R}$  (2 equiv), pyridine or triethylamine (5 equiv),  $\text{CHCl}_3$ , rt, 12 h.

The GK activity was assessed spectrometrically by a coupled reaction with glucose-6-phosphate dehydrogenase (G6PDH).<sup>14–16</sup> Briefly, GK catalyzes glucose phosphorylation to generate glucose-6-P, which was oxidized by the G6PDH with the concomitant reduction of NADP. The product NADPH was then monitored by the increase rate of absorbance at 340 nm in a plate reader (Spectra-Max 190; Molecular Devices, USA). The assay was performed in 96-well plates in a final volume of 100  $\mu\text{L}$  containing 50 mM HEPES pH 7.4, 5 mM glucose, 25 mM KCl, 2 mM  $\text{MgCl}_2$ , 1 mM dithiothreitol (DTT), 1 mM ATP, 1 mM NADP, 2.5 U/mL G6PDH, 0.5  $\mu\text{g}$  (His)<sub>6</sub>-glucokinase. For  $\text{EC}_{50}$  determination, different concentrations of

compounds were tested in the assay, and the fold changes in activity versus controls were fitted to sigmoidal curve using a four-parameter logistic model in GraphPad Prism 4.

### 3.2. Glycogen phosphorylase enzyme assays

Glycogen phosphorylase a (from rabbit muscle), glycogen, glucose-1-phosphate, malachite green, and ammonium molybdate were purchased from the Sigma–Aldrich Corporation (St. Louis, MO, USA). Reagents and solvents were obtained from commercial suppliers and used without further purification. Solvents used were AR grade.

The enzymatic inhibition of phosphorylase activity was monitored using microplate reader (Bio-Rad) based on the published methods.<sup>17</sup> In brief, GP<sub>a</sub> activity was measured in the direction of glycogen synthesis by the release of phosphate from glucose-1-phosphate. Each compound was dissolved in DMSO and diluted at different concentrations for  $\text{IC}_{50}$  determination. The enzymes were added into the 100  $\mu\text{L}$  buffer with compounds dissolved in containing 50 mM Hepes (pH 7.2), 100 mM KCl, 2.5 mM  $\text{MgCl}_2$ , 0.5 mM glucose-1-phosphate, and 1 mg/mL glycogen in 96-well microplates (costar). After the addition of 150  $\mu\text{L}$  of 1 M HCl containing 10 mg/mL ammonium molybdate and 0.38 mg/mL malachite green, reactions were run at  $22^\circ\text{C}$  for 25 min. And then the phosphate absorbance was measured at 655 nm. The  $\text{IC}_{50}$  values were estimated by fitting the inhibition data to a dose-dependent curve using a logistic derivative equation.

## 4. Results and discussion

In this SAR study, we attempted to determine the effect of heteroaryl thiol moiety and the substituted benzyl group based on the central benzamide ring. In addition, according to our previous work, several piperazine-containing amide analogues and symmetrical benzamide analogues with incorporation of substituted benzyl groups were also presented. For a better comparison, we used the GK activator **6** developed by Banyu as the reference compound.

Our previous studies indicated that introducing  $\text{NH}_2$ , CN, F,  $\text{CF}_3$ , and OMe to the phenyl group led to apparent improvement in GP<sub>a</sub> inhibitory activity<sup>11</sup>, we therefore retained these five substitutes. All these substitutions on the phenyl ring turned out to be tolerated in the inhibition of GP<sub>a</sub>. When  $\text{NH}_2$  was introduced, most of the compounds displayed good inhibitory activity. Among these compounds, 1-methyl-1H-imidazole thiol derivative **12** showed the best inhibitory activity while thiazole-2-thiol and 4-methylthiazole-2-thiol derivatives (**13a**, **13b**) had slightly decreased activity.

Pyridine-2-thiol, 1,3,4-thiadiazole-2-thiol and 4,6-dimethylpyrimidine-2-thiol derivatives (**13c–e**) displayed even lower inhibition of GPa activity. The reversed amide analogue **13f** showed decreased activity compared to compound **12**. After inserting a methylene group between the amino nitrogen and the phenyl ring, compound **13g** was slightly less potent to GPa. The CF<sub>3</sub>, F, and CN substituted series with different heteroaryl thiols moieties shared a similar trend in potency change towards GPa: 1-methyl-1*H*-imidazole thiols were more active (**13h**, **13l**, **1q**) while the potency decreased for other heteroaryl thiols. When 3-methoxyl or 4-methoxyl group was introduced, **13v** and **13w** exhibited similarly moderate GPa inhibitory activity. Interestingly, incorporation of 3- and 4-methoxyl groups in the same phenyl ring produced more potent compound **13x** possibly due to increased hydrophobic affinity for GP.

In terms of activation of GK, the variation of heteroaryl thiol moiety indicated a strong preference for 1-methyl-1*H*-imidazole thiol group. Replacing the original 1-methyl-1*H*-imidazole thiol with other heteroaryl thiols had a detrimental effect on activities towards GK. Thiazole-2-thiol substituted benzamides showed weak potency (**13a**, **13i**, **13m**) to GK, while 4-methylthiazole-2-thiols (**13b**, **13j**, **13n**) led to a slight drop in GK activation. Compound **13u** bearing a benzoxazole-2-thiol did not activate GK possibly due to a steric clash between the bulky benzoxazol group and GK enzyme. Compound **13v** was more potent compared to **13w**, indicating the preference for 3-methoxyl over 4-methoxyl group in the phenyl ring. Incorporation of 3- and 4-methoxyl groups in the same phenyl ring afforded increased GK activator **13x** in accordance to the case of GPa inhibition.

In consideration of dual action towards GPa and GK, it turned out that the substituted benzyl group principally accounted for the retainment of GPa inhibitory activity while the heteroaryl thiol moiety was responsible for the activation of GK. From these results, some compounds were proved to be potent GPa inhibitors but with weak potency to GK (**13a**, **13b**, **13e**, **13t**), and some vice versa (**13s**, **13w**). Satisfactorily, there existed analogues within the series that were both potent GPa inhibitors and appreciable GK activators (**12**, **13h**, **13l**, **13q**, **13v**). Compounds **12**, **13h**, **13l**, **13q**, and **13v** demonstrated a good balance of potency to GK and GPa, and were selected for further glucokinase enzyme assay. The EC<sub>50</sub> values against GK were also outlined in Table 1. As shown, **13h** and **13l**, which inhibited GPa with IC<sub>50</sub> values of 8.95 μM and 9.87 μM, showed activation of GK with EC<sub>50</sub> values of 1.87 μM and 2.53 μM, respectively.

The series of piperazine-containing amide analogues exhibited least activities to both GK and GPa, probably due to the semi-flexible moiety of piperazine linker (**14a–e**). The series of symmetrical benzamide analogues displayed no potency primarily due to the rigidity of two amide groups and unfit into the hydrogen bond interactions (**15a–c**) (Table 2).

## 5. Binding model predicted by molecular docking simulation

In order to gain insight into the binding mode of these dual-action compounds against these two targets, molecular simulations were performed by Maestro v8.5 (Schrödinger, Inc.) with Glide-XP (extra-precision). Hydrogen atoms and charges were added during a brief relaxation performed using the Protein Preparation module in Maestro with the 'Preparation and refinement' option. The grid-enclosing box was centered on the centroid of the bound ligand, and a scaling factor of 1.0 was set to Van der Waals (VDW) radii of those receptor atoms with the partial atomic charge less than 0.25. The Glide scoring function (G-Score) was used to select the final ten poses for each ligand. The docking simulations were performed on a Dell Cluster server in parallel.

The crystal structure of RMGP (PDB entry 2IEI) and GK (PDB entry 1V4S) were used in molecular docking simulation. The first ranked docking poses of compounds **12**, **13h**, **13l**, and **13q** were

determined as the preferred binding poses, as shown in Figures 4 and 5. For RMGP case, these compounds bound at the dimmer interface site of RMGP (Fig. 4).<sup>11</sup> For GK case, these compounds were buried in a deep pocket in the hinge region of the enzyme remote from the active site in a manner reminiscent of that reported for GK activator **6** (Fig. 5).<sup>5</sup>

For further and detailed understanding of the binding modes of these compounds with GP and GK, 2D pictures of compound **12**, **13h** and **6** with GP and GK respectively were also created with the program LIGPLOT based on the above docking simulation (Figs. 6 and 7). Hydrogen bonds and hydrophobic interactions between compound **12**, **13h** and **6** with RMGP are exhibited in Figure 6. As indicated, the substituted benzyl group of compound **12** protrudes into the hydrophobic cavity constituted by residues Lys191(A), Val40(B), Trp67(A), Pro229(A) and Trp189(A). The heteroaryl thiol moiety forms hydrophobic contacts with Phe53(B) and His57(B). The carbonyl nitrogen and the amino group of the middle phenyl chelate with the oxygen of Glu190(A). The amino group in substituted benzyl moiety of compound **12** could form another hydrogen bond with Arg60(A). All these interactions may provide stable interactions between these benzamide derivatives and RMGP. Compound **13h** demonstrates a similar binding mode (Fig. 6B) except the loss of a hydrogen bond in the trifluoromethyl phenyl ring, accounting for the decreased inhibitory activity than that of compound **12**.

Figure 7 represents the main interactions between compound **12**, **13h** and **6** with GK. These dual-action compounds bind at the allosteric site of glucokinase. Compound **12** forms hydrophobic contacts with Pro66(A), Val62(A), Val452(A), Ile159(A), Ile211(A), Met235(A), Tyr214(A), and Thr65(A) of glucokinase. The carbonyl oxygen of Arg63(A) and phenolic oxygen of Tyr215(A) anchor the amide NH and amino nitrogen of these compounds respectively with two hydrogen bonds. The only difference of the binding mode of compound **12** and **13h** compared to that of compound **6** is the loss of a hydrogen bond with Arg63(A). The absence of this strong interaction may elucidate the significant decrease in the affinity of these compound for GK with respect to that for compound **6**.

## 6. Conclusions

In summary, we have described the ongoing development of a series of benzamide compounds which can inhibit glycogen phosphorylase *a* and activate glucokinase at the same time. Biochemical evaluation and SAR of these compounds were also conducted. Among these compounds, **12**, **13l**, **13h** and **13q** showed moderate activity towards both GK and GP. The possible binding modes of compounds **12**, **13l**, **13h**, and **13q** with glycogen phosphorylase *a* and glucokinase were also explored by molecular docking simulation.

Based on these results, it can be expected that some reported GK activators or GPa inhibitors may also play a dual role on these two targets simultaneously. These dual actions towards GK and GPa represent a 'double whammy' on the hyperglycemia associated with T2D. The discovery of compounds that act on two targets provides a new methodology to design anti-diabetic agents.

## 7. Experimental

Melting points were measured in capillary tube on a SGW X-4 melting point apparatus without correction. The type of analytical thin-layer chromatography (TLC) was HSGF 254 (0.15–0.2 mm thickness, Yantai Huiyou Company, China). Nuclear magnetic resonance (NMR) spectra were recorded on a Bruker AMX-300 NMR (TMS as IS). Chemical shifts were reported in parts per million

**Table 1**  
Activities of compounds **13a–x** towards GK and GPa

Compound	Structure	GPa IC <sub>50</sub> (μM)	GK fold activation at 10 μM
<b>6</b>		43.9	3.97 (±0.50) <sup>a</sup> EC <sub>50</sub> = 0.06711 μM
<b>12</b>		2.68	2.09 (±0.05) <sup>a</sup> EC <sub>50</sub> = 12.56 μM
<b>13a</b>		5.4	1.21 (±0.08)
<b>13b</b>		3.5	1.10 (±0.11)
<b>13c</b>		17.7	1.22 (±0.09)
<b>13d</b>		10.6	1.12 (±0.10)
<b>13e</b>		9.8	1.09 (±0.06)
<b>13f</b>		28.9	1.16 (±0.04)
<b>13g</b>		25.3	1.01 (±0.13)
<b>13h</b>		8.95	1.47 (±0.03) <sup>a</sup> EC <sub>50</sub> = 1.87 μM
<b>13i</b>		21.1	1.15 (±0.08)
<b>13j</b>		32.5	0.89 (±0.07)
<b>13k</b>		18.9	1.14 (±0.02)

(continued on next page)

Table 1 (continued)

Compound	Structure	GPa IC <sub>50</sub> (μM)	GK fold activation at 10 μM
13l		9.87	1.95 (±0.04) <sup>a</sup> EC <sub>50</sub> = 2.53 μM
13m		34.5	1.20 (±0.13)
13n		18.9	0.99 (±0.10)
13o		44.3	1.20 (±0.10)
13p		19.3	1.01 (±0.04)
13q		30.9	2.04 (±0.04) <sup>a</sup> EC <sub>50</sub> = 2.13 μM
13r		25.9	1.25 (±0.15)
13s		33.6	1.36 (±0.06)
13t		7.2	1.10 (±0.08)
13u		21.6	0.83 (±0.07)
13v		23.9	2.01 (±0.52) <sup>a</sup> EC <sub>50</sub> = 1.36 μM
13w		20.2	1.15 (±0.01)
13x		9.3	1.32 (±0.19)

<sup>a</sup> GK max fold activation.

**Table 2**  
Activities of compounds **14a–e**, **15a–c** towards GK and GPA

Compound	Structure	GPa IC <sub>50</sub> (μM)	GK fold activation at 10 μM
<b>14a</b>		25.8	1.08 (±0.13)
<b>14b</b>		78.5	1.06 (±0.07)
<b>14c</b>		18.7	1.01 (±0.07)
<b>14d</b>		12.5	0.96 (±0.04)
<b>14e</b>		35.9	1.01 (±0.14)
<b>15a</b>		ND <sup>a</sup>	1.02 (±0.13)
<b>15b</b>		77.4	0.81 (±0.08)
<b>15c</b>		ND <sup>a</sup>	0.89 (±0.12)

<sup>a</sup> ND, not determined.

(ppm,  $\delta$ ) downfield from tetramethylsilane. Proton coupling patterns were described as singlet (s), doublet (d), triplet (t), quartet (q), multiplet (m), and broad (br). Low- and high-resolution mass spectra (LRMS and HRMS) were given with electric (EI) produced by Finnigan MAT-95 mass spectrometer.

### 7.1. 2-Amino-*N*-(3-amino-phenyl)-4-fluoro-5-(1-methyl-1*H*-imidazol-2-ylsulfanyl)-benzamide (**12**)

4,5-Difluoro-2-nitrobenzoic acid (200 mg, 0.98 mmol) reacted with oxalyl dichloride (0.2 mL) and DMF (two drops) at room temperature for 2 h. After concentration of the reaction mixture, the residue was dissolved in CH<sub>2</sub>Cl<sub>2</sub> and then added dropwise into the mixture of 3-nitroaniline (91 mg, 0.98 mmol) and pyridine (1.96 mmol) in CH<sub>2</sub>Cl<sub>2</sub>. The mixture was stirred vigorously for 12 h at room temperature and washed with 0.1 M aqueous hydrochloric acid solution (2 × 50 mL), a saturated aqueous sodium bicarbonate solution (2 × 50 mL) and a saturated aqueous sodium chloride solution (2 × 50 mL) sequentially, and then dried over sodium sulfate, filtered, and concentrated in vacuum. A mixture of

the obtained benzamide (190 mg, 0.68 mmol), 1-methyl-1*H*-imidazole-2-thiol (78 mg, 0.68 mmol), and triethylamine (2.05 mmol) in acetonitrile was heated under microwave at 80 °C for 40 min. Upon cooling, the yellow precipitate was filtered and washed with water (5 mL). Then deoxidizing the precipitate by iron powder (2 g) and saturated aqueous NH<sub>4</sub>Cl (2 mL) in isopropanol gave compound **12** as a white solid (157 mg, 45% total yield); mp 144–148 °C; <sup>1</sup>H NMR (DMSO)  $\delta$  7.85 (d, *J* = 7.8 Hz, 1H), 7.25 (s, 1H), 6.95 (t, *J* = 18.9 Hz, 2H), 6.90 (s, 1H), 6.78 (t, *J* = 15.3 Hz, 1H), 6.57 (d, *J* = 11.4 Hz, 1H), 6.31 (d, *J* = 8.1 Hz, 1H), 3.63 (s, 3H); MS (EI, *m/z*) 357 [M]<sup>+</sup>; HRMS (EI) *m/z* calcd for C<sub>17</sub>H<sub>16</sub>FN<sub>5</sub>OS (M<sup>+</sup>) 357.1060, found 357.1052.

### 7.2. 2-Amino-*N*-(3-amino-phenyl)-4-fluoro-5-(thiazol-2-ylsulfanyl)-benzamide (**13a**)

Compound **13a** was prepared as a white solid in a similar manner as described for compound **12**. Yield: 44%; mp 168–172 °C; <sup>1</sup>H NMR (CDCl<sub>3</sub>)  $\delta$  7.99 (br s, 1H), 7.85 (d, *J* = 7.8 Hz, 1H), 7.64 (d, *J* = 3.3 Hz, 1H), 7.20 (d, *J* = 3.3 Hz, 1H), 7.12 (t, *J* = 7.8 Hz, 2H), 6.80

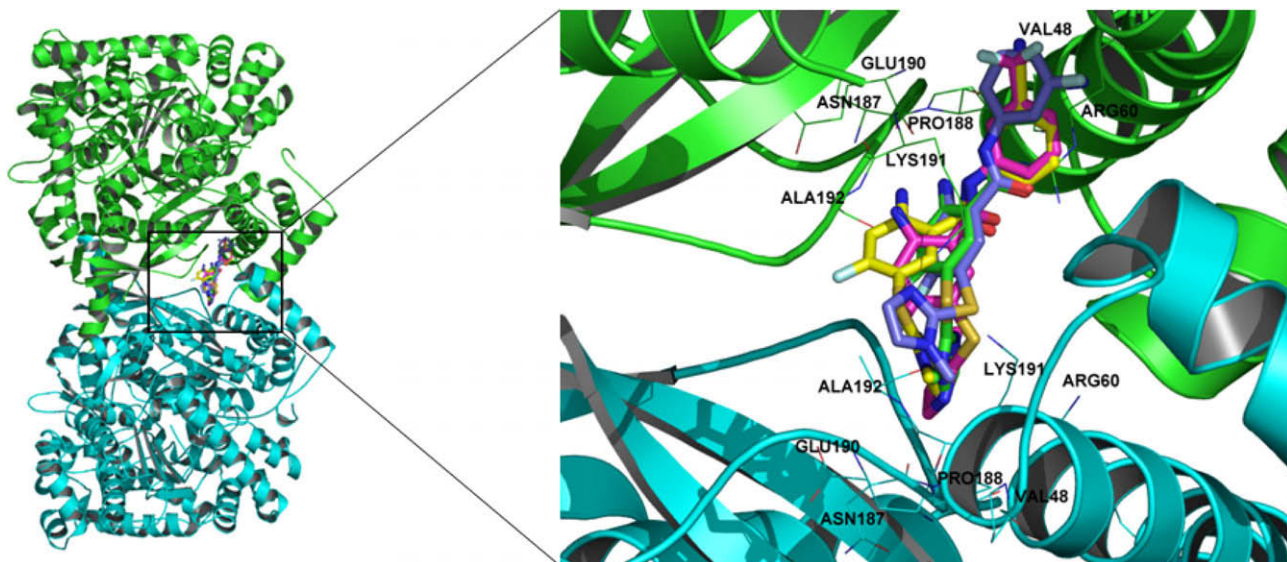


**Figure 4.** Stereoview of the binding poses of compounds **12**, **13h**, **13i**, and **13q** at the dimer interface site of RMGP (left) and enlarged view of binding site (right) with some key residues. The RMGP structure is shown in cartoon (chain A in green and chain B in cyan), and the residues in the binding site are shown in line. The coloring for these compounds is as follows: compound **12** (carbons in green); compound **13h** (carbons in magenta); compound **13i** (carbons in yellow) and compound **13q** (carbons in slate); oxygen atoms, red; nitrogen atoms, blue; sulfur atoms, orange; fluorine, palecyan; respectively. Hydrogen atoms have been omitted for clarity. All structure figures were prepared using PyMol (<http://pymol.sourceforge.net/>).

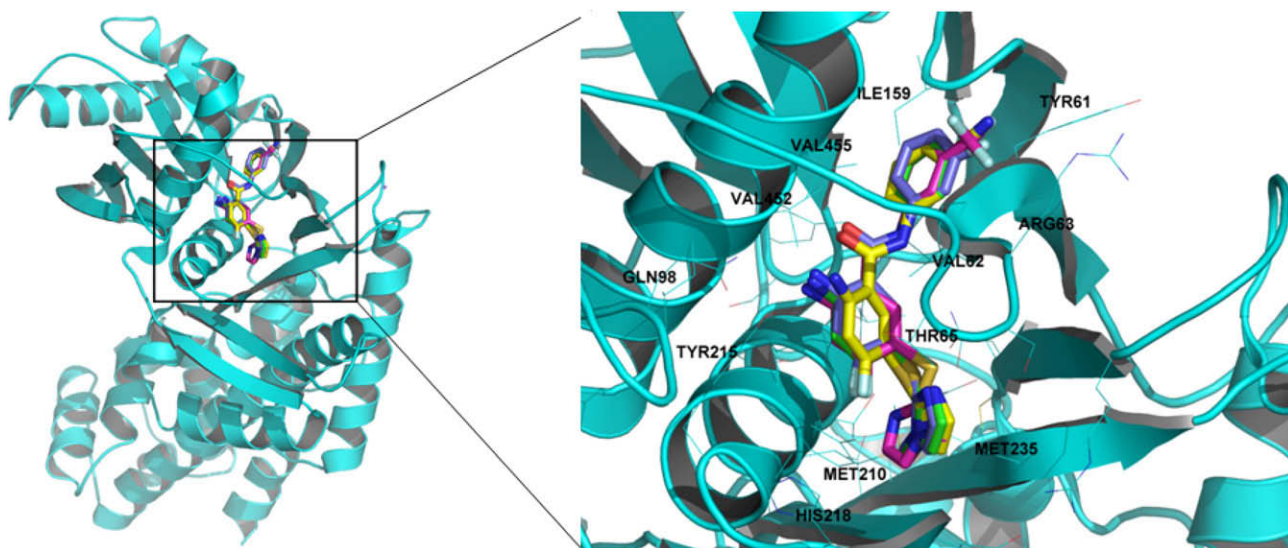


**Figure 5.** Stereoview of the binding poses of compounds **12**, **13h**, **13i**, and **13q** at the allosteric site of glucokinase (left) and enlarged view of allosteric site (right) with some key residues. The GK structure is shown in cartoon and the residues in the binding site are shown in line. The coloring for these compounds is as follows: compound **12** (carbons in green); compound **13h** (carbons in magenta); compound **13i** (carbons in yellow) and compound **13q** (carbons in slate); oxygen atoms, red; nitrogen atoms, blue; sulfur atoms, orange; fluorine, palecyan; respectively. Hydrogen atoms have been omitted for clarity.

(d,  $J = 7.5$  Hz, 1H), 6.48 (d,  $J = 10.2$  Hz, 2H), 6.10 (br s, 2H); MS (EI,  $m/z$ ) 360 [M]<sup>+</sup>; HRMS (EI) calcd for C<sub>16</sub>H<sub>13</sub>OS<sub>2</sub>N<sub>4</sub>F [M]<sup>+</sup> 360.0515, found 360.0523.

### 7.3. 2-Amino-N-(3-amino-phenyl)-4-fluoro-5-(4-methyl-thiazol-2-ylsulfanyl)-benzamide (**13b**)

Compound **13b** was prepared as a white solid in a similar manner as described for compound **12**. Yield: 59%; mp 175–178 °C; <sup>1</sup>H NMR (DMSO)  $\delta$  10.36 (s, 1H), 9.86 (s, 1H), 8.12 (d,  $J = 8.1$  Hz, 1H), 7.24 (s, 1H), 7.11 (s, 1H), 7.00 (s, 1H), 6.95 (d,  $J = 8.4$  Hz, 1H), 6.80

(d,  $J = 7.2$  Hz, 1H), 6.71 (d,  $J = 11.4$  Hz, 1H), 6.33 (d,  $J = 8.1$  Hz, 1H), 5.22 (br s, 2H), 2.29 (s, 3H); MS (EI,  $m/z$ ) 374 [M]<sup>+</sup>; HRMS (EI) calcd for C<sub>17</sub>H<sub>15</sub>OS<sub>2</sub>N<sub>4</sub>F [M]<sup>+</sup> 374.0671, found 374.0687.

### 7.4. 2-Amino-N-(3-amino-phenyl)-4-fluoro-5-(1,3,4-thiadiazol-2-ylsulfanyl)-benzamide (**13c**)

Compound **13c** was prepared as a white solid in a similar manner as described for compound **12**. Yield: 49%; mp 228 °C; <sup>1</sup>H NMR (DMSO)  $\delta$  9.85 (s, 1H), 9.46 (s, 1H), 8.17 (d,  $J = 8.1$  Hz, 1H), 7.29 (s, 2H), 6.98 (s, 1H), 6.96 (t,  $J = 8.1$  Hz, 1H), 6.79 (d,  $J = 9.0$  Hz, 1H), 6.73

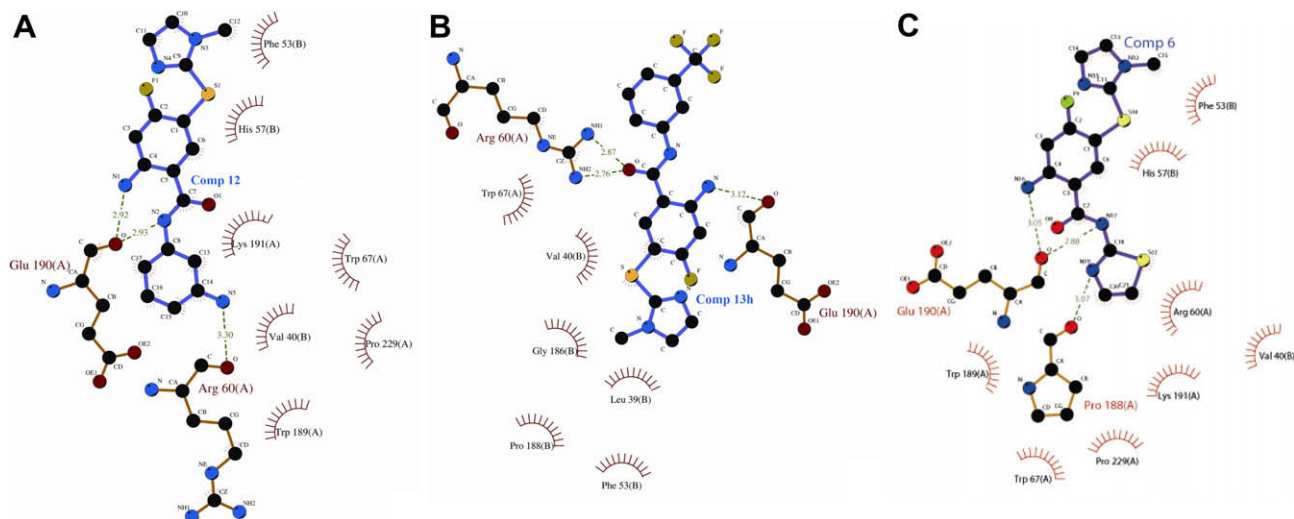


**Figure 6.** Two-dimensional representations for the interacting modes of compounds **12** (A), **13h** (B) and **6** (C) with GP. Dotted lines represent the hydrogen bonds and the half circles represent the hydrophobic contacts. The hydrogen bonds and hydrophobic interactions were calculated by LIGPLOT.<sup>18</sup>

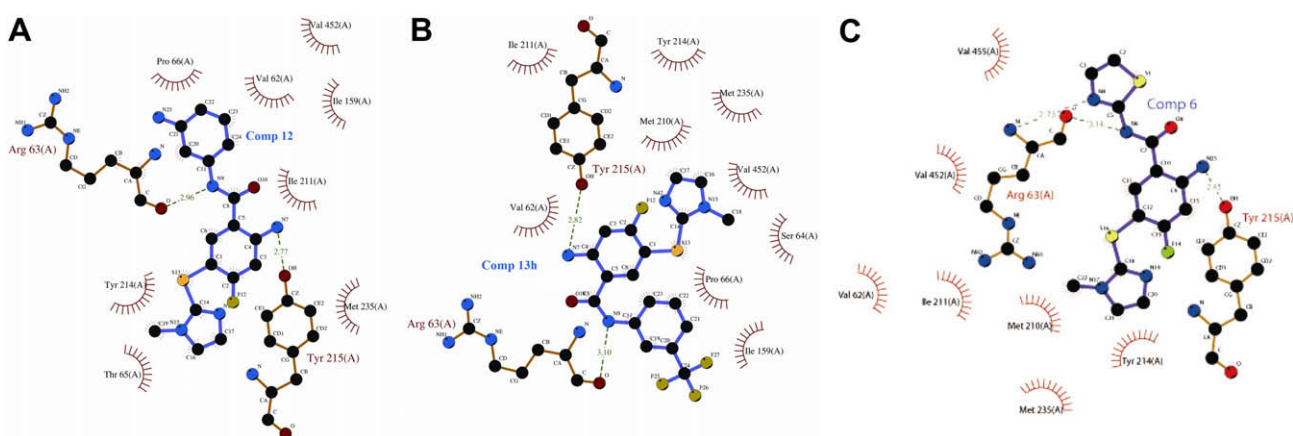


**Figure 7.** Two-dimensional representations for the interacting modes of compounds **12** (A), **13h** (B) and **6** (C) with GK. Dotted lines represent the hydrogen bonds and the half circles represent the hydrophobic contacts. The hydrogen bonds and hydrophobic interactions were calculated by LIGPLOT.<sup>18</sup>

(d,  $J = 11.7$  Hz, 1H), 6.32 (d,  $J = 8.4$  Hz, 1H), 5.08 (s, 2H); MS (EI,  $m/z$ ) 361 [M]<sup>+</sup>; HRMS (EI) calcd for C<sub>15</sub>H<sub>12</sub>OS<sub>2</sub>N<sub>5</sub>F [M]<sup>+</sup> 361.0467, found 361.0472.

#### 7.5. 2-Amino-*N*-(3-amino-phenyl)-4-fluoro-5-(pyridin-2-ylsulfanyl)-benzamide (**13d**)

Compound **13d** was prepared as a white solid in a similar manner as described for compound **12**. Yield: 35%; mp 180–182 °C; <sup>1</sup>H NMR (DMSO)  $\delta$  9.89 (s, 1H), 8.43 (s, 1H), 8.04 (d,  $J = 8.1$  Hz, 1H), 7.70 (t,  $J = 6.9$  Hz, 1H), 7.15 (s, 3H), 7.04 (s, 1H), 7.00 (s, 1H), 6.98 (s, 1H), 6.83 (d,  $J = 8.4$  Hz, 1H), 6.74 (d,  $J = 11.1$  Hz, 1H), 6.36 (d,  $J = 7.5$  Hz, 1H), 5.16 (br s, 2H); MS (EI,  $m/z$ ) 354 [M]<sup>+</sup>; HRMS (EI) calcd for C<sub>18</sub>H<sub>15</sub>OSN<sub>4</sub>F [M]<sup>+</sup> 354.0951, found 354.0960.

#### 7.6. 2-Amino-*N*-(3-amino-phenyl)-5-(4,6-dimethyl-pyrimidin-2-ylsulfanyl)-4-fluoro-benzamide (**13e**)

Compound **13e** was prepared as a white solid in a similar manner as described for compound **12**. Yield: 61%; mp 115–118 °C; <sup>1</sup>H NMR (DMSO)  $\delta$  9.81 (s, 1H), 7.91 (d,  $J = 7.5$  Hz, 1H), 7.03–6.90 (m, 5H), 6.76 (d,  $J = 8.1$  Hz, 1H), 6.63 (d,  $J = 12.0$  Hz, 1H), 6.29 (d,

$J = 7.5$  Hz, 1H), 5.06 (s, 2H), 2.28 (s, 6H); MS (EI,  $m/z$ ) 383 [M]<sup>+</sup>; HRMS (EI) calcd for C<sub>19</sub>H<sub>18</sub>OSN<sub>5</sub>F [M]<sup>+</sup> 383.1216, found 383.1225.

#### 7.7. 3-Amino-*N*-[2-amino-4-fluoro-5-(1-methyl-1*H*-imidazol-2-ylsulfanyl)-phenyl]-benzamide (**13f**)

Compound **13f** was prepared as a white solid in a similar manner as described for compound **12**. Yield: 48%; mp 202–205 °C; <sup>1</sup>H NMR (DMSO)  $\delta$  9.42 (s, 1H), 7.29 (s, 1H), 7.15–7.09 (m, 4H), 6.92 (s, 1H), 6.73 (d,  $J = 7.5$ , 1H), 6.59 (d,  $J = 7.5$ , 1H), 5.46 (s, 2H), 5.27 (s, 2H), 3.66 (s, 3 Hz); MS (EI,  $m/z$ ) 357 [M]<sup>+</sup>; HRMS (EI) calcd for C<sub>17</sub>H<sub>16</sub>OSN<sub>5</sub>F [M]<sup>+</sup> 357.1060, found 357.1050.

#### 7.8. 2-Amino-*N*-(3-aminomethyl-phenyl)-4-fluoro-5-(1-methyl-1*H*-imidazol-2-ylsulfanyl)-benzamide (**13g**)

Compound **13g** was prepared as a white solid in a similar manner as described for compound **12**. Yield: 46%; mp 80–83 °C; <sup>1</sup>H NMR (DMSO)  $\delta$  10.15 (s, 1H), 7.93 (d,  $J = 8.1$  Hz, 1H), 7.68 (s, 1H), 7.53 (d,  $J = 8.1$  Hz, 1H), 7.27 (s, 1H), 7.09 (d,  $J = 8.1$  Hz, 1H), 6.92 (s, 1H), 6.89 (s, 1H), 6.57 (d,  $J = 11.7$  Hz, 1H), 3.77 (s, 2H); MS (EI,

$m/z$  371 [M]<sup>+</sup>; HRMS (EI) calcd for C<sub>18</sub>H<sub>18</sub>OSN<sub>5</sub>F [M]<sup>+</sup> 371.1216, found 371.1215.

### 7.9. 2-Amino-4-fluoro-5-(1-methyl-1H-imidazol-2-ylsulfanyl)-N-(3-trifluoromethyl-phenyl)-benzamide (13h)

Compound **13h** was prepared as a white solid in a similar manner as described for compound **12**. Yield: 34%; mp 95–100 °C; <sup>1</sup>H NMR (DMSO) δ 8.13 (s, 1H), 7.90–7.97 (m, 2H), 7.56 (t,  $J = 16.5$  Hz, 1H), 7.42 (d,  $J = 7.8$  Hz, 1H), 7.25 (s, 1H), 6.89 (s, 1H), 6.58 (d,  $J = 11.7$  Hz, 1H), 3.66 (s, 3H); MS (EI,  $m/z$ ) 410 [M]<sup>+</sup>; HRMS (EI)  $m/z$  calcd for C<sub>18</sub>H<sub>14</sub>F<sub>4</sub>N<sub>4</sub>OS (M<sup>+</sup>) 410.0824, found 410.0818.

### 7.10. 2-Amino-4-fluoro-5-(thiazol-2-ylsulfanyl)-N-(3-trifluoromethyl-phenyl)-benzamide (13i)

Compound **13i** was prepared as a white solid in a similar manner as described for compound **12**. Yield: 66%; mp 182–183 °C; <sup>1</sup>H NMR (DMSO) δ 10.42 (br s, 1H), 8.23 (d,  $J = 8.1$  Hz, 1H), 8.16 (s, 1H), 7.97 (d,  $J = 8.1$  Hz, 1H), 7.68 (d,  $J = 3.6$  Hz, 1H), 7.58 (dd,  $J = 9.0$ , 5.7 Hz, 2H), 7.44 (d,  $J = 8.1$  Hz, 1H), 7.34 (s, 1H), 6.75 (d,  $J = 11.4$  Hz, 1H); MS (EI,  $m/z$ ) 413 [M]<sup>+</sup>; HRMS (EI) calcd for C<sub>17</sub>H<sub>11</sub>OS<sub>2</sub>N<sub>3</sub>F<sub>4</sub> [M]<sup>+</sup> 413.0280, found 413.0285.

### 7.11. 2-Amino-4-fluoro-5-(4-methyl-thiazol-2-ylsulfanyl)-N-(3-trifluoromethyl-phenyl)-benzamide (13j)

Compound **13j** was prepared as a white solid in a similar manner as described for compound **12**. Yield: 57%; mp 183–185 °C; <sup>1</sup>H NMR (DMSO) δ 10.48 (br s, 1H), 8.26 (d,  $J = 7.8$  Hz, 1H), 8.18 (s, 1H), 7.99 (d,  $J = 7.8$  Hz, 1H), 7.58 (t,  $J = 7.8$  Hz, 1H), 7.44 (d,  $J = 8.1$  Hz, 1H), 7.37 (s, 1H), 7.11 (s, 1H), 6.78 (d,  $J = 11.7$  Hz, 1H), 2.29 (s, 3H); MS (EI,  $m/z$ ) 427 [M]<sup>+</sup>; HRMS (EI) calcd for C<sub>18</sub>H<sub>13</sub>OS<sub>2</sub>N<sub>3</sub>F<sub>4</sub> [M]<sup>+</sup> 427.0436, found 427.0451.

### 7.12. 2-Amino-4-fluoro-5-(1,3,4-thiadiazol-2-ylsulfanyl)-N-(3-trifluoromethyl-phenyl)-benzamide (13k)

Compound **13k** was prepared as a white solid in a similar manner as described for compound **12**. Yield: 61%; mp 193 °C; <sup>1</sup>H NMR (DMSO) δ 10.38 (br s, 1H), 9.47 (br s, 1H), 8.26 (d,  $J = 8.1$  Hz, 1H), 8.16 (s, 1H), 7.96 (d,  $J = 7.8$  Hz, 1H), 7.59 (t,  $J = 7.8$  Hz, 1H), 7.45 (d,  $J = 7.5$  Hz, 1H), 7.37 (s, 2H), 6.77 (d,  $J = 11.7$  Hz, 1H); MS (EI,  $m/z$ ) 414 [M]<sup>+</sup>; HRMS (EI) calcd for C<sub>16</sub>H<sub>10</sub>OS<sub>2</sub>N<sub>4</sub>F<sub>4</sub> [M]<sup>+</sup> 414.0232, found 414.0229.

### 7.13. 2-Amino-N-(3-cyano-phenyl)-4-fluoro-5-(1-methyl-1H-imidazol-2-ylsulfanyl)-benzamide (13l)

Compound **13l** was prepared as a white solid in a similar manner as described for compound **12**. Yield: 55%; mp 172–174 °C; <sup>1</sup>H NMR (DMSO) δ 7.92 (d,  $J = 8.0$  Hz, 1H), 7.84 (s, 1H), 7.68 (d,  $J = 8.3$  Hz, 1H), 7.34 (t,  $J = 16.3$  Hz, 1H), 7.24 (s, 1H), 7.18 (d,  $J = 7.3$  Hz, 1H), 6.88 (s, 1H), 6.57 (d,  $J = 11.7$  Hz, 1H), 3.66 (s, 3H); MS (EI,  $m/z$ ) 367 [M]<sup>+</sup>; HRMS (EI)  $m/z$  calcd for C<sub>18</sub>H<sub>14</sub>FN<sub>5</sub>OS (M<sup>+</sup>) 367.0903, found 367.0977.

### 7.14. 2-Amino-N-(3-cyano-phenyl)-4-fluoro-5-(thiazol-2-ylsulfanyl)-benzamide (13m)

Compound **13m** was prepared as a white solid in a similar manner as described for compound **12**. Yield: 30%; mp 213–215 °C; <sup>1</sup>H NMR (DMSO) δ 10.38 (s, 1H), 8.21 (d,  $J = 8.1$  Hz, 1H), 8.17 (s, 1H), 7.95 (br, 1H), 7.68 (d,  $J = 3.0$  Hz, 1H), 7.58 (d,  $J = 3.0$  Hz, 1H), 7.56

(d,  $J = 4.5$  Hz, 1H), 7.32 (s, 2H), 6.75 (d,  $J = 11.7$  Hz, 1H); MS (EI,  $m/z$ ) 370 [M]<sup>+</sup>; HRMS (EI) calcd for C<sub>17</sub>H<sub>11</sub>FN<sub>4</sub>OS<sub>2</sub> [M]<sup>+</sup> 370.0358, found 370.0357.

### 7.15. 2-Amino-N-(3-cyano-phenyl)-4-fluoro-5-(4-methyl-thiazol-2-ylsulfanyl)-benzamide (13n)

Compound **13n** was prepared as a white solid in a similar manner as described for compound **12**. Yield: 45%; mp 162–166 °C; <sup>1</sup>H NMR (DMSO) δ 8.19 (s, 1H), 8.17 (s, 1H), 7.96 (br, 1H), 7.61–7.55 (m, 3H), 7.10 (s, 1H), 6.75 (d,  $J = 11.7$  Hz, 1H), 3.29 (s, 3H); MS (EI,  $m/z$ ) 384 [M]<sup>+</sup>; HRMS (EI) calcd for C<sub>18</sub>H<sub>13</sub>FN<sub>4</sub>OS<sub>2</sub> [M]<sup>+</sup> 384.0515, found 384.0508.

### 7.16. 2-Amino-N-(3-cyano-phenyl)-4-fluoro-5-(1,3,4-thiadiazol-2-ylsulfanyl)-benzamide (13o)

Compound **13o** was prepared as a white solid in a similar manner as described for compound **12**. Yield: 55%; mp 213–216 °C; <sup>1</sup>H NMR (DMSO) δ 10.39 (s, 1H), 9.47 (s, 1H), 8.23 (d,  $J = 8.1$  Hz, 1H), 8.17 (s, 1H), 7.94 (br, 1H), 7.57 (d,  $J = 5.1$  Hz, 2H), 7.36 (s, 2H), 6.76 (d,  $J = 11.7$  Hz, 1H); MS (EI,  $m/z$ ) 371 [M]<sup>+</sup>; HRMS (EI) calcd for C<sub>16</sub>H<sub>10</sub>FN<sub>5</sub>OS<sub>2</sub> [M]<sup>+</sup> 371.0311, found 371.0309.

### 7.17. 2-Amino-N-(3-cyano-phenyl)-5-(4,6-dimethyl-pyrimidin-2-ylsulfanyl)-4-fluoro-benzamide (13p)

Compound **13p** was prepared as a white solid in a similar manner as described for compound **12**. Yield: 57%; mp 246 °C; <sup>1</sup>H NMR (DMSO) δ 10.36 (s, 1H), 8.17 (s, 1H), 7.99 (d,  $J = 7.8$  Hz, 1H), 7.96 (m, 1H), 7.55 (d,  $J = 5.1$  Hz, 2H), 7.13 (s, 1H), 6.98 (s, 1H), 6.67 (d,  $J = 11.7$  Hz, 1H), 2.29 (s, 6H); MS (EI,  $m/z$ ) 393 [M]<sup>+</sup>; HRMS (EI) calcd for C<sub>20</sub>H<sub>16</sub>FN<sub>5</sub>OS [M]<sup>+</sup> 393.1060, found 393.1052.

### 7.18. 2-Amino-4-fluoro-N-(3-fluoro-phenyl)-5-(1-methyl-1H-imidazol-2-ylsulfanyl)-benzamide (13q)

Compound **13q** was prepared as a white solid in a similar manner as described for compound **12**. Yield: 49%; mp 190–193 °C; <sup>1</sup>H NMR (CD<sub>3</sub>OD) δ 7.92 (d,  $J = 7.5$  Hz, 1H), 7.64 (d,  $J = 11.7$  Hz, 1H), 7.46 (d,  $J = 7.5$  Hz, 1H), 7.35–7.40 (m, 1H), 7.25 (s, 1H), 6.90–6.94 (m, 2H), 6.59 (d,  $J = 11.7$  Hz, 1H), 3.68 (s, 3H); MS (EI,  $m/z$ ) 360 [M]<sup>+</sup>; HRMS (EI)  $m/z$  calcd for C<sub>17</sub>H<sub>14</sub>F<sub>2</sub>N<sub>4</sub>OS (M<sup>+</sup>) 360.0856, found 360.0833.

### 7.19. 2-Amino-4-fluoro-N-(3-fluoro-phenyl)-5-(thiazol-2-ylsulfanyl)-benzamide (13r)

Compound **13r** was prepared as a white solid in a similar manner as described for compound **12**. Yield: 36%; <sup>1</sup>H NMR (DMSO) δ 10.27 (s, 1H), 8.17 (d,  $J = 8.4$  Hz, 1H), 7.68 (d,  $J = 3.3$  Hz, 1H), 7.64 (s, 1H), 7.57 (d,  $J = 3.3$  Hz, 1H), 7.47 (d,  $J = 8.1$  Hz, 1H), 7.36 (dd,  $J = 15.0$ , 8.1 Hz, 1H), 7.29 (s, 1H), 6.92 (td,  $J = 9.0$ , 2.7 Hz, 1H), 6.73 (d,  $J = 11.7$  Hz, 1H); MS (EI,  $m/z$ ) 363 [M]<sup>+</sup>; HRMS (EI) calcd for C<sub>16</sub>H<sub>11</sub>F<sub>2</sub>N<sub>3</sub>OS<sub>2</sub> [M]<sup>+</sup> 363.0312, found 363.0311.

### 7.20. 2-Amino-4-fluoro-N-(3-fluoro-phenyl)-5-(1,3,4-thiadiazol-2-ylsulfanyl)-benzamide (13s)

Compound **13s** was prepared as a white solid in a similar manner as described for compound **12**. Yield: 43%; mp 215–218 °C; <sup>1</sup>H NMR (DMSO) δ 10.28 (s, 1H), 9.46 (s, 1H), 8.20 (d,  $J = 8.1$  Hz, 1H),

7.65 (d,  $J = 12.0$  Hz, 1H), 7.48–7.33 (m, 4H), 6.93 (t,  $J = 7.8$  Hz, 1H), 6.75 (d,  $J = 11.7$  Hz, 1H); MS (EI,  $m/z$ ) 364 [M]<sup>+</sup>; HRMS (EI) calcd for C<sub>15</sub>H<sub>10</sub>F<sub>2</sub>N<sub>4</sub>O<sub>5</sub> [M]<sup>+</sup> 364.0246, found 364.0258.

#### 7.21. 2-Amino-4-fluoro-*N*-(3-fluoro-phenyl)-5-(pyridin-2-ylsulfanyl)-benzamide (13t)

Compound **13t** was prepared as a white solid in a similar manner as described for compound **12**. Yield: 38%; mp 183–185 °C; <sup>1</sup>H NMR (DMSO)  $\delta$  10.25 (s, 1H), 8.37 (d,  $J = 3.9$  Hz, 1H), 8.05 (d,  $J = 7.8$  Hz, 1H), 7.67 (d,  $J = 7.8$  Hz, 1H), 7.64 (s, 1H), 7.48 (d,  $J = 8.4$  Hz, 1H), 7.36 (dd,  $J = 12.0, 7.8$  Hz, 1H), 7.13 (m, 2H), 6.93 (m, 2H), 6.72 (d,  $J = 12.0$  Hz, 1H); MS (EI,  $m/z$ ) 357 [M]<sup>+</sup>; HRMS (EI) calcd for C<sub>18</sub>H<sub>13</sub>F<sub>2</sub>N<sub>3</sub>O<sub>5</sub> [M]<sup>+</sup> 357.0747, found 357.0755.

#### 7.22. 2-Amino-5-(benzoxazol-2-ylsulfanyl)-4-fluoro-*N*-(3-fluoro-phenyl)-benzamide (13u)

Compound **13u** was prepared as a white solid in a similar manner as described for compound **12**. Yield: 23%; mp 190–194 °C; <sup>1</sup>H NMR (DMSO)  $\delta$  10.30 (s, 1H), 8.16 (d,  $J = 7.8$  Hz, 1H), 7.68–7.61 (m, 2H), 7.48–7.26 (m, 6H), 6.92 (t,  $J = 9.0$  Hz, 1H), 6.76 (d,  $J = 11.4$  Hz, 1H); MS (EI,  $m/z$ ) 397 [M]<sup>+</sup>; HRMS (EI) calcd for C<sub>20</sub>H<sub>13</sub>F<sub>2</sub>N<sub>3</sub>O<sub>2</sub>S [M]<sup>+</sup> 397.0697, found 397.0698.

#### 7.23. 2-Amino-4-fluoro-*N*-(4-methoxy-phenyl)-5-(1-methyl-1H-imidazol-2-ylsulfanyl)-benzamide (13v)

Compound **13v** was prepared as a white solid in a similar manner as described for compound **12**. Yield: 22%; mp 95–100 °C; <sup>1</sup>H NMR (300 Hz, CD<sub>3</sub>OD)  $\delta$  7.91 (d,  $J = 8.1$  Hz, 1H), 7.51 (d,  $J = 9.0$  Hz, 2H), 7.17 (s, 1H), 6.99 (s, 1H), 6.92 (d,  $J = 9.3$  Hz, 2H), 6.49 (d,  $J = 11.7$  Hz, 1H), 3.80 (d,  $J = 2.1$  Hz, 6H); MS (EI,  $m/z$ ) 372 [M]<sup>+</sup>; HRMS (EI)  $m/z$  calcd for C<sub>18</sub>H<sub>17</sub>FN<sub>4</sub>O<sub>2</sub>S (M<sup>+</sup>) 372.1056, found 372.1056.

#### 7.24. 2-Amino-4-fluoro-*N*-(3-methoxy-phenyl)-5-(1-methyl-1H-imidazol-2-ylsulfanyl)-benzamide (13w)

Compound **13w** was prepared as a white solid in a similar manner as described for compound **12**. Yield: 32%; mp 72–73 °C; <sup>1</sup>H NMR (300 Hz, DMSO)  $\delta$  7.95 (d,  $J = 8.0$  Hz, 1H), 7.40 (s, 1H), 7.27–7.30 (m, 3H), 6.94 (s, 1H), 6.72 (d,  $J = 7.2$  Hz, 1H), 6.63 (d,  $J = 11.7$  Hz, 1H), 3.78 (s, 3H), 3.72 (s, 3H); MS (EI,  $m/z$ ) 372 [M]<sup>+</sup>; HRMS (EI)  $m/z$  calcd for C<sub>18</sub>H<sub>17</sub>FN<sub>4</sub>O<sub>2</sub>S (M<sup>+</sup>) 372.1056, found 372.1059.

#### 7.25. 2-Amino-*N*-(3,4-dimethoxy-phenyl)-4-fluoro-5-(1-methyl-1H-imidazol-2-ylsulfanyl)-benzamide (13x)

Compound **13x** was prepared as a white solid in a similar manner as described for compound **12**. Yield: 63%; mp 101–104 °C; <sup>1</sup>H NMR (DMSO)  $\delta$  10.01 (s, 1H), 7.91 (d,  $J = 8.1$  Hz, 1H), 7.35 (s, 1H), 7.26 (s, 1H), 7.23 (d,  $J = 8.1$  Hz, 1H), 6.91 (m, 3H), 6.57 (d,  $J = 11.7$  Hz, 1H), 3.75 (s, 3H), 3.74 (s, 3H), 3.35 (s, 3H); MS (EI,  $m/z$ ) 402 [M]<sup>+</sup>; HRMS (EI) calcd for C<sub>19</sub>H<sub>19</sub>FN<sub>4</sub>O<sub>3</sub>S [M]<sup>+</sup> 402.1162, found 402.1166.

#### 7.26. *N*-(3-Amino-phenyl)-2-[4-(2-fluoro-phenyl)-piperazin-1-yl]-acetamide (14a)

A solution of 3-nitroaniline (276 mg, 2 mmol) and anhydrous potassium carbonate (415 mg, 3 mmol) in THF (20 mL) was added

with 2-chloroacetyl chloride (339 mg, 3 mmol) dropwise. Then the mixture was stirred under reflux for 2 h. After evaporation THF, the residue was dissolved with water and the precipitate was collected by filtration. A mixture of the obtained acetamide (232 mg, 1.32 mmol), 1-(2-fluorophenyl)piperazine (213 mg, 1.32 mmol), and anhydrous potassium carbonate (273 mg, 1.98 mmol) in THF was reacted under reflux for 4 h using potassium iodide as catalyst. The reaction mixture was evaporated and water was added subsequently, and then the pH value was adjusted to neutral using 1 M aqueous hydrochloric acid solution. 2-[4-(2-Fluoro-phenyl)-piperazin-1-yl]-*N*-(3-nitro-phenyl)-acetamide was collected by filtration, water washing, and purification by flash column chromatography. The obtained acetamide was then dissolved in methanol (20 mL) containing 10% palladium on carbon (25 mg) and the suspension was stirred in an atmosphere of hydrogen for 2 h. The catalyst was then filtered and the solvent evaporated. Compound **14a** was obtained as a white solid by flash column chromatography. Yield: 67%; mp 121–123 °C; <sup>1</sup>H NMR (DMSO)  $\delta$  9.42 (s, 1H), 7.16–7.05 (m, 3H), 7.02–6.89 (m, 3H), 6.71 (d,  $J = 7.8$  Hz, 1H), 6.28 (d,  $J = 7.5$  Hz, 1H), 5.07 (br s, 2H), 3.15 (s, 2H), 3.07 (t,  $J = 4.5$  Hz, 4H), 2.68 (t,  $J = 4.2$  Hz, 4H); MS (EI,  $m/z$ ) 328 [M]<sup>+</sup>; HRMS (EI) calcd for C<sub>18</sub>H<sub>21</sub>FN<sub>4</sub>O [M]<sup>+</sup> 328.1699, found 381.1701.

#### 7.27. 2-[4-(2-Fluoro-phenyl)-piperazin-1-yl]-*N*-(3-trifluoromethyl-phenyl)-acetamide (14b)

Compound **14b** was prepared as a white solid in a similar manner as described for compound **14a**. Yield: 75%; mp 93–95 °C; <sup>1</sup>H NMR (DMSO)  $\delta$  8.16 (s, 1H), 7.90 (d,  $J = 8.3$  Hz, 1H), 7.56 (t,  $J = 15.6$  Hz, 1H), 7.41 (d,  $J = 7.7$  Hz, 1H), 7.05–7.16 (m, 3H), 6.95–6.99 (m, 1H), 3.24 (s, 2H), 3.09 (t,  $J = 9.2$  Hz, 4H), 2.70 (t,  $J = 8.8$  Hz, 4H); MS (EI,  $m/z$ ) 381 [M]<sup>+</sup>; HRMS (EI)  $m/z$  calcd for C<sub>19</sub>H<sub>19</sub>F<sub>4</sub>N<sub>3</sub>O (M<sup>+</sup>) 381.1464, found 381.1472.

#### 7.28. *N*-(3-Fluoro-phenyl)-2-[4-(2-fluoro-phenyl)-piperazin-1-yl]-acetamide (14c)

Compound **14c** was prepared as a white solid in a similar manner as described for compound **14a**. Yield: 77%; mp 100–101 °C; <sup>1</sup>H NMR (DMSO)  $\delta$  9.98 (s, 1H), 7.64 (d,  $J = 12.0$  Hz, 1H), 7.42–7.30 (m, 2H), 7.16 (m, 5H), 3.21 (s, 2H), 3.08 (t,  $J = 4.2$  Hz, 4H), 2.68 (t,  $J = 4.5$  Hz, 4H); MS (EI,  $m/z$ ) 331 [M]<sup>+</sup>; HRMS (EI) calcd for C<sub>18</sub>H<sub>19</sub>F<sub>2</sub>N<sub>3</sub>O [M]<sup>+</sup> 331.1496, found 331.1501.

#### 7.29. *N*-(3-Cyano-phenyl)-2-[4-(2-fluoro-phenyl)-piperazin-1-yl]-acetamide (14d)

Compound **14d** was prepared as a white solid in a similar manner as described for compound **14a**. Yield: 71%; mp 140–141 °C; <sup>1</sup>H NMR (DMSO)  $\delta$  10.11 (s, 1H), 8.16 (s, 1H), 7.95 (s, 1H), 7.53 (d,  $J = 4.5$  Hz, 2H), 7.16–6.96 (m, 4H), 3.24 (s, 2H), 3.09 (s, 4H), 2.69 (s, 4H); MS (EI,  $m/z$ ) 338 [M]<sup>+</sup>; HRMS (EI) calcd for C<sub>19</sub>H<sub>19</sub>FN<sub>4</sub>O [M]<sup>+</sup> 338.1543, found 338.1554.

#### 7.30. 2-[4-(2,4-Difluoro-phenyl)-piperazin-1-yl]-*N*-(3,4-dimethoxy-phenyl)-acetamide (14e)

Compound **14e** was prepared as a white solid in a similar manner as described for compound **14a**. Yield: 69%; mp 142–145 °C; <sup>1</sup>H NMR (CDCl<sub>3</sub>)  $\delta$  9.59 (s, 1H), 7.34 (d,  $J = 2.4$  Hz, 1H), 7.23–7.15 (m, 2H), 7.13–6.96 (m, 3H), 6.88 (d,  $J = 8.7$  Hz, 1H), 3.73 (s, 3H), 3.72 (s, 3H), 3.17 (s, 2H), 3.04 (t,  $J = 4.5$  Hz, 4H), 2.68 (t,  $J = 4.5$  Hz, 4H); MS (EI,  $m/z$ ) 391 [M]<sup>+</sup>; HRMS (EI) calcd for C<sub>20</sub>H<sub>23</sub>F<sub>2</sub>N<sub>3</sub>O<sub>3</sub> [M]<sup>+</sup> 391.1707, found 391.1709.

### 7.31. *N,N'*-Bis-(2-methoxy-phenyl)-isophthalamide (**15a**)

To a solution of 2-methoxyaniline (123 mg, 1 mmol) and pyridine (2.5 mmol) in  $\text{CHCl}_3$  (10 mL) was added isophthaloyl dichloride (82 mg, 0.5 mmol) dropwise. After the mixture was stirred overnight, a saturated aqueous sodium bicarbonate solution (5 mL) was added in and reacted for another 30 min. Then compound **15a** was collected by filtration, water washing, and purification as a white solid. Yield: 82%; mp 173–176 °C;  $^1\text{H}$  NMR ( $\text{CDCl}_3$ )  $\delta$  8.63 (s, 2H, 8.52 (dd,  $J = 6.0, 1.5$  Hz, 2H), 8.42 (t  $J = 1.2$  Hz, 1H), 8.08 (dd,  $J = 6.0, 1.8$  Hz, 2H), 7.64 (t,  $J = 7.8$  Hz, 1H), 7.12 (t,  $J = 7.1$  Hz, 2H), 7.04 (t,  $J = 6.3$  Hz, 2H), 6.94 (d,  $J = 7.8$  Hz, 2H), 3.94 (s, 6H); MS (EI,  $m/z$ ) 376  $[\text{M}]^+$ ; HRMS (EI) calcd for  $\text{C}_{22}\text{H}_{20}\text{N}_2\text{O}_4$   $[\text{M}]^+$  376.1423, found 376.1421.

### 7.32. *N,N'*-Bis-(3-methoxy-phenyl)-isophthalamide (**15b**)

Compound **15b** was prepared as a white solid in a similar manner as described for compound **15a**. Yield: 83%; mp 302–303 °C;  $^1\text{H}$  NMR (DMSO)  $\delta$  10.39 (s, 2H), 8.51 (s, 1H), 8.14 (d,  $J = 7.8$  Hz, 2H), 7.69 (t,  $J = 7.5$  Hz, 1H), 7.49 (s, 2H), 7.40 (d,  $J = 7.8$  Hz, 2H), 7.27 (t,  $J = 8.1$  Hz, 2H), 6.71 (dd,  $J = 7.8, 2.1$  Hz, 2H), 3.77 (s, 6H); MS (EI,  $m/z$ ) 376  $[\text{M}]^+$ ; HRMS (EI) calcd for  $\text{C}_{22}\text{H}_{20}\text{N}_2\text{O}_4$   $[\text{M}]^+$  376.1423, found 376.1428.

### 7.33. *N,N'*-Bis-(4-methoxy-phenyl)-isophthalamide (**15c**)

Compound **15c** was prepared as a white solid in a similar manner as described for compound **15a**. Yield: 79%; mp 242–245 °C;  $^1\text{H}$  NMR (DMSO)  $\delta$  10.29 (s, 2H), 8.50 (s, 1H), 8.11 (dd,  $J = 7.5, 1.2$  Hz, 2H), 7.71–7.64 (m, 5H), 6.94 (m, 4H), 3.75 (6H, s); MS (EI,  $m/z$ ) 376  $[\text{M}]^+$ ; HRMS (EI) calcd for  $\text{C}_{22}\text{H}_{20}\text{N}_2\text{O}_4$   $[\text{M}]^+$  376.1423, found 376.1419.

### Acknowledgments

We gratefully acknowledge generous support from the National Natural Science Foundation of China (Grants 20372069, 29725203, 20803022, and 20472094), the Basic Research Project for Talent Research Group from the Shanghai Science and Technology Commission, the Key Project from the Shanghai Science and Technology Commission (Grant 02DJ14006), the Key Project for New Drug Re-

search from CAS, and the 863 Hi-Tech Program of China (Grants 2006AA020402, 2006AA020602).

### Supplementary data

Supplementary data associated with this article can be found, in the online version, at doi:10.1016/j.bmc.2009.08.045.

### References and notes

- Hampson, L. J.; Arden, C.; Agius, L.; Ganotidis, M.; Kosmopoulou, M. N.; Tiraidis, C.; Elemen, Y.; Sakarellos, C.; Leonidas, D. D.; Oikonomakos, N. G. *Bioorg. Med. Chem.* **2006**, *14*, 7835.
- Matschinsky, F. M. *Diabetes* **1996**, *45*, 223.
- Matschinsky, F. M. *Diabetes* **2002**, *51*, S394.
- (a) Pal, M. *Drug Discovery Today*, in press, doi:10.1016/j.drudis.2009.05.013.; (b) Coghlan, M.; Leighton, B. *Exp. Opin. Invest. Drugs* **2008**, *17*, 145; (c) Sarabu, R.; Taub, R.; Grimsby, J. *Drug Discovery Today: Therapeutic Strategies* **2007**, *4*, 111; (d) Guertin, K. R.; Grimsby, J. *Curr. Med. Chem.* **2006**, *13*, 1839; (e) Johnson, T. O.; Humphries, P. S.; Anthony, W. In *Annual Reports in Medicinal Chemistry*; Academic Press, 2006; Vol. 41. p 141.
- Kamata, K.; Mitsuya, M.; Nishimura, T.; Eiki, J.; Nagata, Y. *Structure* **2004**, *12*, 429.
- Kristiansen, M.; Andersen, B.; Iversen, L. F.; Westergaard, N. J. *Med. Chem.* **2004**, *47*, 3537.
- Oikonomakos, N. G.; Tiraidis, C.; Leonidas, D. D.; Zographos, S. E.; Kristiansen, M.; Jessen, C. U.; Norskov-Lauritsen, L.; Agius, L. *J. Med. Chem.* **2006**, *49*, 5687.
- Treadway, J. L.; Mendys, P.; Hoover, D. J. *Exp. Opin. Invest. Drugs* **2001**, *10*, 439.
- Oikonomakos, N. G.; Somsák, L. *Curr. Opin. Invest. Drugs* **2008**, *9*, 9379.
- Henke, B. R.; Sparks, S. M. *Mini-Rev. Med. Chem.* **2006**, *6*, 845.
- Chen, L.; Li, H.; Liu, J.; Zhang, L.; Liu, H.; Jiang, H. *Bioorg. Med. Chem.* **2007**, *15*, 6763.
- Harwood, H. J.; Petras, S. F.; Hoover, D. J.; Mankowski, D. C.; Soliman, V. F.; Sugarman, E. D.; Hulin, B.; Kwon, Y.; Gibbs, E. M.; Mayne, J. T.; Treadway, J. L. *J. Lipid Res.* **2005**, *46*, 547.
- Futamura, M.; Hosaka, H.; Kadotani, A.; Shimazaki, H.; Sasaki, K.; Ohya, S.; Nishimura, T.; Eiki, J.; Nagata, Y. *J. Biol. Chem.* **2006**, *281*, 37668.
- Brocklehurst, K. J.; Payne, V. A.; Davies, R. A.; Carroll, D.; Vertigan, H. L.; Wightman, H. J.; Aiston, S.; Waddell, I. D.; Leighton, B.; Coghlan, M. P.; Agius, L. *Diabetes* **2004**, *53*, 535.
- Efanov, A. M.; Barrett, D. G.; Brenner, M. B.; Briggs, S. L.; Delaunois, A.; Durbin, J. D.; Giese, U.; Guo, H.; Radloff, M.; Gil, G. S.; Sewing, S.; Wang, Y.; Weichert, A.; Zaliani, A.; Gromada, J. *Endocrinology* **2005**, *146*, 3696.
- Fyfe, M. C. T.; White, J. R.; Taylor, A.; Chatfield, R.; Wargent, E.; Printz, R. L.; Sulpice, T.; McCormack, J. G.; Procter, M. J.; Reynet, C.; Widdowson, P. S.; Wong-Kai-In, P. *Diabetologia* **2007**, *50*, 1277.
- Martin, W. H.; Hoover, D. J.; Armento, S. J.; Stock, I. A.; McPherson, R. K.; Danley, D. E.; Stevenson, R. W.; Barrett, E. J.; Treadway, J. L. *Proc. Natl. Acad. Sci. U.S.A.* **1998**, *95*, 1776.
- Wallace, A. C.; Laskowski, R. A.; Thornton, J. M. *Protein Eng.* **1995**, *8*, 127.